International Journal of Minerals, Metallurgy and Materials
Volume 21, Number 11, November 2014, Page 1115
DOI: 10.1007/s12613-014-1016-4

Characteristics of alumina particles in dispersion-strengthened copper alloys

Xue-hui Zhang[1)] *and Xiao-xian Li*[2)]

1) School of Materials Science and Engineering, Jiangxi University of Science and Technology, Ganzhou 341000, China

2) School of Metallurgical and Chemical Engineering, Jiangxi University of Science and Technology, Ganzhou 341000, China

(Received: 18 February 2014; revised: 15 May 2014; accepted: 20 May 2014)

Abstract: Two types of alumina dispersion-strengthened copper (ADSC) alloys were fabricated by a novel *in-situ* reactive synthesis (IRS) and a traditional internal oxidation (IO) process. The features of alumina dispersoids in these ADSC alloys were investigated by X-ray diffraction, scanning electron microscopy, and high-resolution transmission electron microscopy. It is found that nano-sized γ-Al_2O_3 particles of approximately 10 nm in diameter are homogeneously distributed in the IRS-ADSC composites. Meanwhile, larger-sized, mixed crystal structure alumina with rod-shaped morphology is embedded in the IO-ADSC alloy. The IRS-ADSC composites can obtain better mechanical and physical properties than the IO-ADSC composites; the tensile strength of the IRS-ADSC alloy can reach 570 MPa at room temperature, its electrical conductivity is 85% IACS, and the Rockwell hardness can reach 86 HRB.

Keywords: metallic matrix composites; alumina; copper; *in-situ* reactive synthesis; internal oxidation

1. Introduction

Alumina dispersion-strengthened copper (ADSC) alloys are a family of metallic matrix composites by using nano-scale alumina ceramic particles uniformly distributed in a copper matrix as a strengthening phase [1–3]. Alumina ceramic particles have been selected as a strengthening phase due to their advantages such as favorable thermal and chemical stability, high melting point and high hardness [4]. These particles can efficiently pin dislocations and impede the movement of grain boundaries. Moreover, they can also inhibit recrystallization and grain growth. For these reasons, ADSC alloys exhibit the excellent properties of high strength and high electrical conductivity at both ambient and elevated temperatures [5–7].

At present, ADSC alloys can be prepared by various powder metallurgy methods such as internal oxidation (IO), reactive spray deposition (RSD), mechanical alloying (MA), and *in-situ* reactive synthesis (IRS) [8–10]. However, the traditional IO process uses solid-phase cuprous oxide as an oxygen source for the selective oxidation of aluminum at elevated temperatures in a gas shielded or sealed container. This process involves significant shortcomings that need to be improved; for example, coarse cuprous oxide cannot be completely reduced to copper and remains in the copper matrix, seriously affecting the performance of the ADSC alloys. In addition, the complexity of the traditional IO process makes the quality of ADSC alloys difficult to control. The IRS method is a promising approach to produce high-quality ADSC alloys; it involves chemical reactions between additives and alloyed powders with the help of external actions [11]. If nano-sized Al_2O_3 particles can be obtained and dispersed homogeneously inside the copper matrix, the resultant pinning effect on dislocations, sub-grains and grains can increase the strength and hardness of ADSC alloys at elevated temperatures. In recent years, studies on ADSC alloys have focused mainly on the effects of various strengthening particles and preparation processes on alloy properties [12–13]; however, a systematic investigation on the characteristics of alumina particles in ADSC alloys is absent.

In this paper, two techniques were used to fabricate ADSC alloys: a novel IRS process and a traditional IO process. The phase structure, size, morphology, and distribution of alumina particles dispersed in the produced ADSC

Corresponding author: Xue-hui Zhang E-mail: zxh312264585@163.com

alloys were comparatively investigated.

2. Experimental

Previous procedures for the IRS and IO processes were the same. Cu–0.6wt%Al alloy powders were fabricated by water atomization followed by drying and sieving. The IO process utilized cuprous oxide or high-purity nitrogen mixed with oxygen as oxidants for the selective oxidation of Cu–Al alloy powders at elevated temperatures in a gas-shielded or sealed container. In the IRS process, a new oxidant and the atomized Cu–Al powders were used as raw materials. The IRS process was then performed by chemical reactions between the additive and the Cu–Al powders in a gas-sealed polyurethane container at room temperature. Cu–1.12wt%Al_2O_3 powders used in both the IRS and IO process were heat treated in a hydrogen protective atmosphere at 973 K for 60 min followed by cold isostatic pressing into a columnar billet. The forming pressure and dwell time were 200 MPa and 10 min, respectively. The compacted powders were sintered at 1193 K for 60 min and hot-extruded at a ratio of 20:1 to fabricate a 14-mm diameter bar. These two ADSC composites are both produced by General Research Institute for Nonferrous Metals (GRINM).

If all aluminum in Cu–0.6wt%Al alloy powders is completely oxidized into alumina, the weight percent of alumina will be about 1.12wt%. Nano-sized alumina particles with such low volume fractions in the copper matrix cannot be detected by normal X-ray diffraction (XRD) methods. Thus, it is necessary to collect these particles by extraction, which was conducted on the basis of the Chinese standard "Atomizing Copper Powder" (YS/T 499—2006). Identification of the phase structures of the dispersoids extracted from IRS-ADSC and IO-ADSC alloys were performed using an X'Pert PRO MPD X-ray diffractometer with Cu $K_{\alpha 1}$ radiation. The scanning ranges were taken from 10° to 90° in the step of $\Delta 2\theta$ = 0.033°. Meanwhile, the morphologies of particles extracted from ADSC alloys were investigated and analyzed using field emission scanning electron microscopy (FE-SEM; JSM-7001F) and high resolution transmission electron microscopy (HRTEM; JEM-2010; accelerating voltage of 200 kV).

3. Results and discussion

3.1. XRD patterns of alumina particles

The phase structure of alumina can be detected using XRD. Fig. 1 shows the XRD patterns of dispersoids extracted from IRS-ADSC and IO-ADSC alloys. Only the fcc phase of γ-Al_2O_3 is detected in the IRS-ADSC alloy (Fig. 1(a)). The broadened diffraction peaks indicate that the grains of γ-Al_2O_3 are refined. The XRD pattern of alumina extracted from the IO-ADSC alloy reveals α-Al_2O_3, γ-Al_2O_3, and θ-Al_2O_3 phase structures (Fig. 1(b)) with α-Al_2O_3 as the main structure. A comparison of diffraction peak widths demonstrates that the average grain size of alumina extracted from the IO-ADSC alloy is much larger than that extracted from the IRS-ADSC alloy .

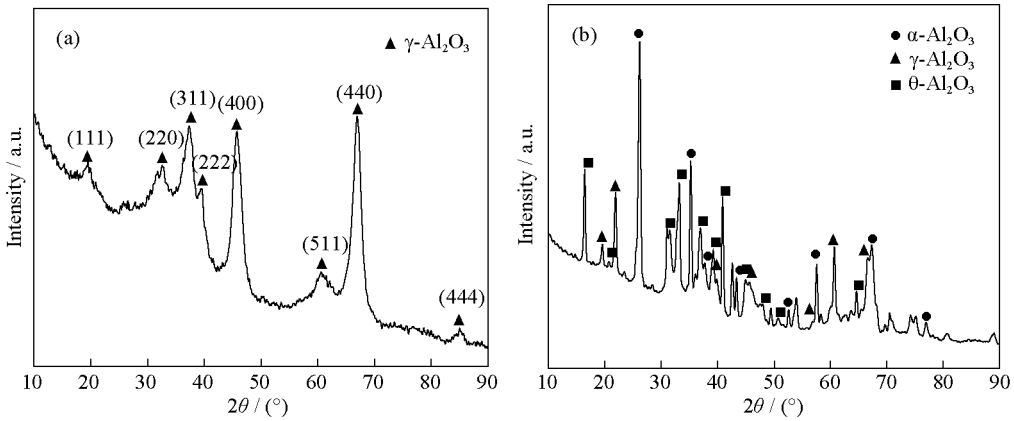

Fig. 1. XRD patterns of dispersoids extracted from (a) IRS-ADSC and (b) IO-ADSC composites.

3.2. Morphologies and microstructures of alumina particles

Fig. 2 shows the SEM images of alumina dispersoids extracted from the prepared ADSC alloys. Alumina dispersoids extracted from the IRS-ADSC alloy present nearly spherical morphologies with small dimensions under several nanometers (Fig. 2(a)). The morphologies of alumina dispersoids extracted from the IO-ADSC alloy are clusters consisting of large numbers of clavate-shaped particles. These clavate-shaped particles have dimensions exceeding 100 nm and can reach 600 nm in length. Fig. 3 shows TEM

images of alumina particles extracted from the IRS-ADSC and IO-ADSC alloys. Again, it can be seen that the grain size of alumina particles extracted from the IRS-ADSC alloy is on the order of several nanometers (Fig. 3(a)), while that of IO-ADSC alumina ranges from 50 to 600 nm (Fig. 3(b)). The maximum length of the clavate-shaped alumina particles determined by TEM (Fig. 3(c)) is 630 nm. The existence of such large alumina particles in the copper matrix will seriously damage the performance of the alloy. Furthermore, all the ring patterns of the IRS-ADSC alumina dispersoids in the selected-area diffraction pattern (SADP, inset of Fig. 3(a)) belong to γ-Al_2O_3, while the coarse alumina particle is α-Al_2O_3 (inset of Fig. 3(c)). The SADP results are in perfect agreement with the results of the XRD analysis.

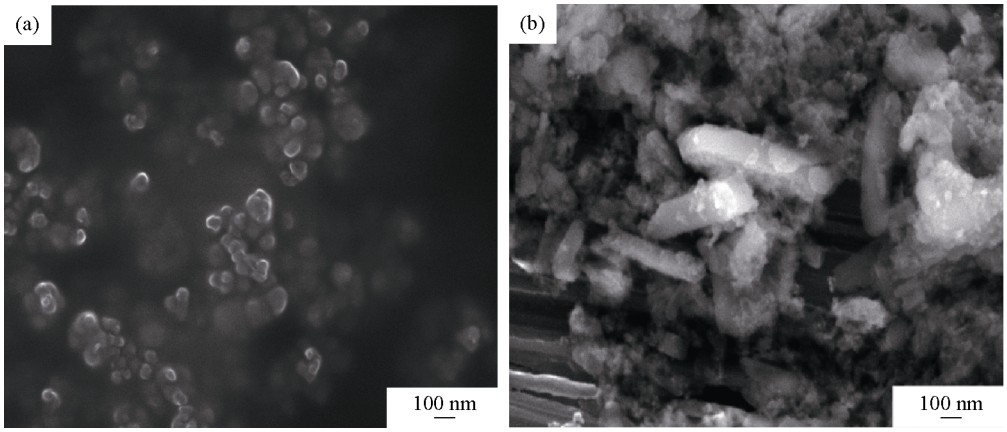

Fig. 2. SEM images of alumina dispersoids extracted from IRS-ADSC (a) and IO-ADSC alloys (b).

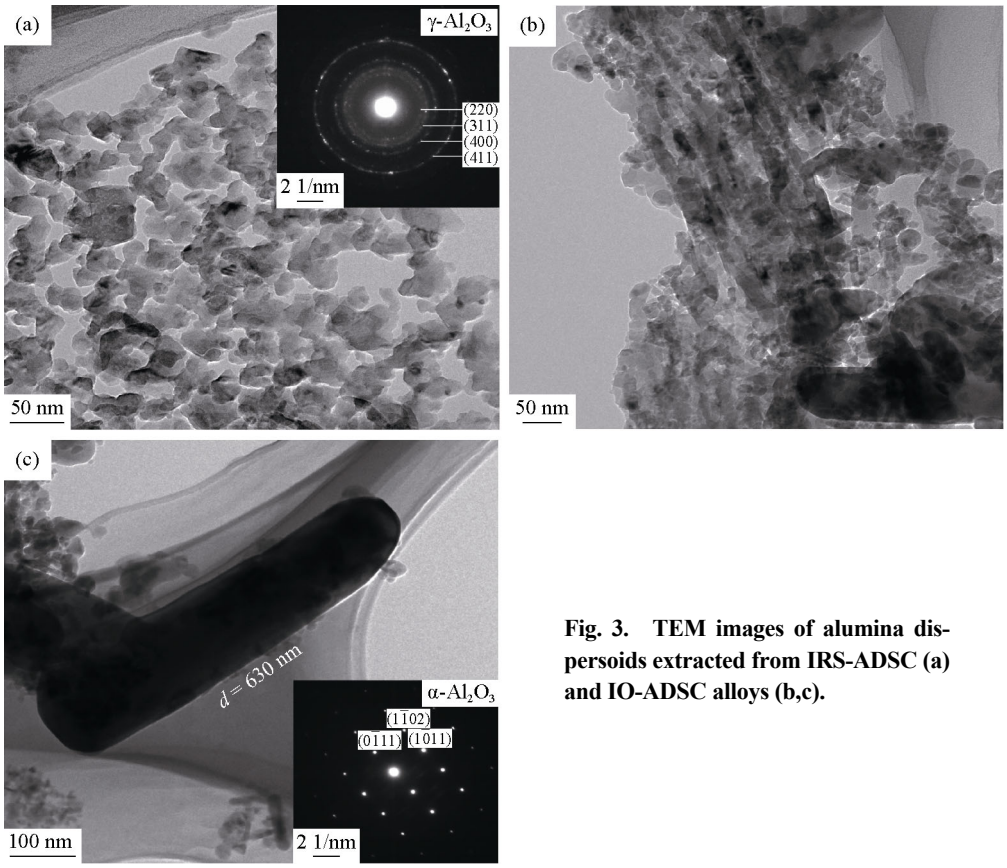

Fig. 3. TEM images of alumina dispersoids extracted from IRS-ADSC (a) and IO-ADSC alloys (b,c).

Fig. 4 shows a TEM image of fine alumina particles distributed in the hot-extruded IRS-ADSC alloy. The mean grain size of the copper matrix is in the range of 150 to 300 nm. The fine alumina phase with a mean particle diameter

of approximately 10 nm is uniformly distributed in the copper matrix. According to the Orowan strengthening mechanism [14–15], nano-sized alumina particles homogenously dispersed in the copper matrix can effectively pin dislocation movement and impede grain boundary sliding (Fig. 4(b)). Such an effect can obviously improve the strength of the alloy.

3.3. Performances

Table 1 gives the mechanical properties and electrical conductivity values of the ADSC samples prepared by the IRS process along with the commercial Glidcop® Al-60 alloy fabricated by the traditional IO method for comparison. Tensile test results shown in Table 1 are the averages of three measurements, and the other values were obtained from five measurements. The tensile properties and electrical conductivity associated with the IRS process are higher than those of the IO process. Remarkably, the Rockwell hardness of the alloy prepared by the IRS process can reach up to 86 HRB, which is significantly higher than that obtained with the IO process. According to the Orowan strengthening mechanism and the fine grain strengthening theory [16–17], tiny alumina particles distributed uniformly in the copper matrix can hinder dislocation motion and improve the strength of the composite material. As the sizes of the alumina particles and copper grains decrease, the dislocation blocking effect is enhanced and the overall strengthening effect on the composite becomes more notable.

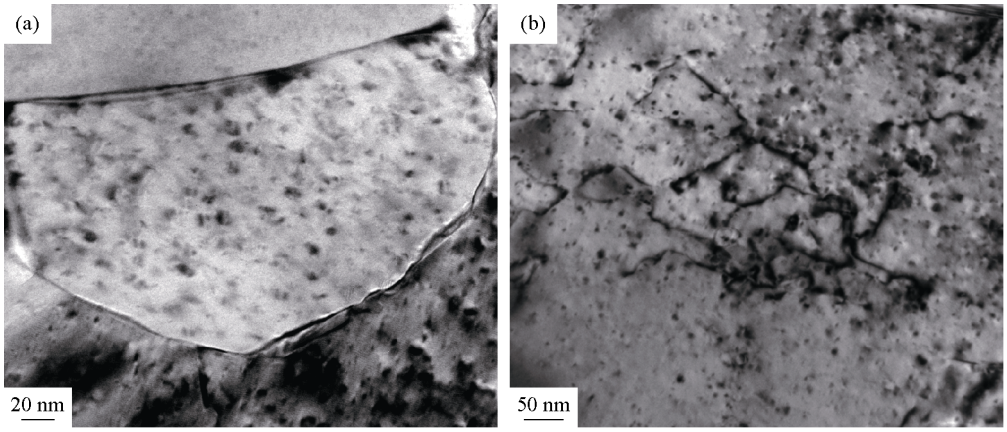

Fig. 4. Alumina particles distributed in the copper matrix (a) and pinning of dislocations (b).

Table 1. Comparison between the properties of ADSC composites prepared by IRS and IO processes

Process	Tensile strength / MPa	Rockwell hardness, HRB	Electrical conductivity / % IACS
IRS	570	86	85
IO	551	80	78

4. Conclusions

A comparative investigation on the characteristics of alumina particles dispersed in IRS-ADSC and IO-ADSC alloys was conducted. The following conclusions can be drawn:

(1) Only nearly spherical γ-Al_2O_3 particles with diameters of approximately 10 nm are homogeneously distributed in the copper matrix of the IRS-ADSC composite, and these particles easily form a coherent interface with the copper matrix.

(2) Alumina particles with mixed crystal structures, α-Al_2O_3 phase structures, and rod-shaped morphologies are embedded in the IO-ADSC alloy. Their dimensions exceed 50 nm, with a maximum length of 630 nm.

(3) The IRS-ADSC composites possess better mechanical and physical properties than the IO-ADSC composites. The tensile strength of the IRS-ADSC alloy can reach 570 MPa at room temperature. The electrical conductivity is 85% IACS, and the Rockwell hardness can reach up to 86 HRB.

Acknowledgements

This work is financially supported by the National Natural Science Foundation of China (NO. 51464013) and the Dr. Initialization Fund of Jiangxi University of Science and Technology (No. jxxjbs14013).

References

[1] V. Rajkovic, D. Bozic, A. Devecerski, and M.T. Jovanovic, Characteristic of copper matrix simultaneously reinforced with nano- and micro-sized Al_2O_3 particles, *Mater. Charact.*, 67(2012), p. 129.

[2] K. Ďurišinová, J. Ďurišin, and M. Orolínová, Al_2O_3-dispersion strengthened nanocrystalline copper, *Powder Metall. Prog.*, 6(2006), No. 2, p. 75.

[3] P.K. Jena, E.A. Brocchi, I.G. Solórzano, and M.S. Motta, Identification of a third phase in Cu–Al_2O_3 nanocomposites prepared by chemical routes, *Mater. Sci. Eng. A*, 371(2004), No. 1-2, p. 72.

[4] R.A. Espinoza, R.H. Palma, A.O. Sepúlveda, V. Fuenzalida, G. Solórzano, A. Craievich, D.J. Smith, T. Fujita, and M. López, Microstructural characterization of dispersion-strengthened Cu–Ti–Al alloys obtained by reaction milling, *Mater. Sci. Eng. A*, 454-455(2007), p. 183.

[5] B.H. Tian, P. Liu, K.X. Song, Y. Li, Y. Liu, F.Z. Ren, and J.H. Su, Microstructure and properties at elevated temperature of a nano-Al_2O_3 particles dispersion-strengthened copper base composite, *Mater. Sci. Eng. A*, 435-436(2006), p. 705.

[6] F. Shehata, A. Fathy, M. Abdelhameed, and S.F. Moustafa, Preparation and properties of Al_2O_3 nanoparticle reinforced copper matrix composites by in situ processing, *Mater. Des*., 30(2009), No. 7, p. 2756.

[7] J.P. Stobrawa and Z.M. Rdzawski, Dispersion-strengthened nanocrystalline copper, *J. Achiev. Mater. Manuf. Eng*., 24(2007), No. 2, p. 35.

[8] S.L. Han, X.D. Qin, Y.X. Cai, K. Luo, H.W. Xie, and D.R. Li, Properties and fabrication of alumina dispersion strengthened copper alloy with high softening temperature, *Mater. Sci. Forum*, 749(2013), p. 425.

[9] R. Wu, D.W. Zhang, J. Sun, F.Z. Ren, and Q.C. He, Preparation of Al_2O_3/Cu composites by internal oxidation in Cu–Al alloy sheet processing, *Adv. Mater. Res*., 602-604(2013), p. 2034.

[10] X.H. Zhang, C.G. Lin, S. Cui, and Z.D. Li, Microstructure and properties of Al_2O_3 dispersion-strengthened copper fabricated by reactive synthesis process, *Rare Met*., 33(2014), No. 2, p. 191.

[11] X.H. Zhang, C.G. Lin, S. Cui, Z.D. Li, and X.K. Hu, Microstructure of Al_2O_3-dispersion strengthened copper prepared by SPS, *Trans. Mater. Heat Treat.*, 34(2013), No. 11, p. 1.

[12] N. Valibeygloo, R.A. Khosroshahi, and R.T. Mousavian, Microstructural and mechanical properties of Al–4.5wt%Cu reinforced with alumina nanoparticles by stir casting method, *Int. J. Miner. Metall. Mater.*, 20(2013), No. 10, p. 978.

[13] J.H. Nie, C.C. Jia, X. Jia, Y. Li, Y.F. Zhang, and X.B. Liang, Fabrication and thermal conductivity of copper matrix composites reinforced by tungsten-coated carbon nanotubes, *Int. J. Miner. Metall. Mater.*, 19(2012), No. 5, p. 446.

[14] D.V. Kudashov, H. Baum, U. Martin, M. Heilmaier, and H. Oettel, Microstructure and room temperature hardening of ultra-fine-grained oxide-dispersion strengthened copper prepared by cryomilling, *Mater. Sci. Eng. A*, 387-389(2004), p. 768.

[15] H.R. Palma and O.A. Sepúlveda, Contamination effects on precipitation hardening of Cu–alumina alloys, prepared by mechanical alloying, *Mater. Sci. Forum*, 416-418(2003), p. 162.

[16] P. Yan, C.G. Lin, S. Cui, Y.J. Lu, Z.L. Zhou, and Z.D. Li, Microstructural features and properties of high-hardness and heat-resistant dispersion strengthened copper by reaction milling, *J. Wuhan Univ. Technol. Mater. Sci. Ed*., 26(2011), No. 5, p. 902.

[17] J.Y. Cheng, M.P. Wang, J.G. Cao, X.L. Zhao, and M.X. Guo, Influence of nano-scaled dispersed second phase on substructure of deformed dispersion strengthened copper alloy, *J. Cent. South Univ. Technol.*, 12(2005), No. 1, p. 50.